ON ALGORITHMS AND IMPLEMENTATIONS OF A 4-CHANNEL ACTIVE NOISE CANCELING WINDOW

Chuang Shi, Nan Jiang, Huiyong Li

School of Electronic Engineering,
University of Electronic Science and
Technology of China, Chengdu, China

Dongyuan Shi, Woon-Seng Gan

School of Electrical and Electronic Engineering,
Nanyang Technological University,
Singapore

ABSTRACT

The active noise canceling window is an application of the multi-channel active noise control (ANC) system, which aims to provide a quiet living environment while preserving the ventilation of the room. In the implementation of the active noise canceling window, the standard multiple-error LMS algorithm demands too much computational power to be handled by a common digital signal processor (DSP). Hence, the minimax algorithm, which minimize the amplitude instead of the power of the noise field, is revisited. The minimax algorithm is compared with the multiple-error LMS algorithm based on numerical simulations of a case (1, 4, 4) ANC system and real-time experiments with floating-point implementations. The simulation and experiment results show that the minimax algorithm has a distinct advantage in reducing the computational complexity but its trade-off is the relatively slow convergence speed.

Index Terms— Active noise control, minimax algorithm, multiple-error LMS algorithm, active noise canceling window

1. INTRODUCTION

The history of the active noise control (ANC) technology can be traced back to 1936, when Lueg was granted the patent on the "process of silencing sound oscillations", whereby a reference signal was used to generate the control signal and the quiet zone was formed behind the secondary loudspeaker [1]. This is now widely known as the feedforward structure of ANC systems. In the 1980s, the emergence of adaptive signal processing and digital signal processors (DSPs) accelerated the development of the ANC technology. In the early 1990s, Eriksson reported the successful implementation of an ANC system to deal with the noise in an air duct [2]. From then on, ANC systems have been widely used in many noise mitigating applications [3, 4, 5].

This material is based on research work jointly supported by the National Science Foundation of China (Grant No. 61671137), the Fundamental Research Funds for the Central Universities (Project No. A03017023601291), and the Singapore Ministry of National Development and National Research Foundation (L2 NIC Award No. L2NICCFP1-2013-7).

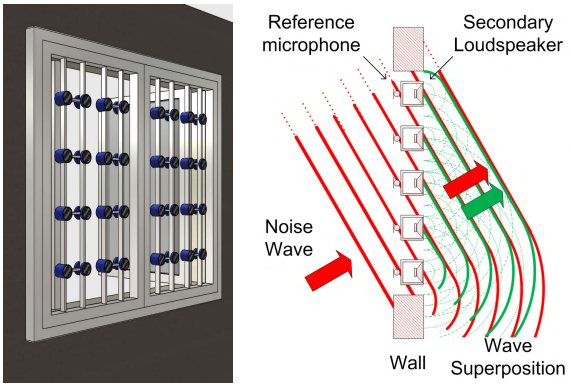

Fig. 1. Illustration of the active noise canceling window (pictures are extracted from [6, 7]).

Some of the ANC applications focus on the local cancellation of noise, typically within one tenth of the noise wavelength from the error microphone, while multi-channel ANC systems are necessarily deployed when the targeted control areas are large. The computational complexity of a multi-channel feedforward ANC system increases with the numbers of reference microphones, secondary loudspeakers, and error microphones [7]. Active control of noise in large 3D spaces is therefore more complicated and costly [8]. Since successful implementation of ANC systems is dependent on their practicality, different approaches to reduce the computational complexity have been attempted, such as the collocated and decentralized systematic configurations [9, 10].

Active noise canceling window is an application of the multi-channel ANC system to provide a quiet living environment while preserving the ventilation of the room [11]. According to Ise's boundary surface control principle, the sound field in an enclosed space can be controlled by adjusting the sound pressure and particle velocity on the surface of the space [12]. Therefore, the active noise canceling window is feasible to generate an anti-noise field with inverted phase of the noise field, so that the noise level in the room is globally minimized, as illustrated in Fig. 1.

This paper works on a demo setup of the active noise canceling window, which consists of two by two feedforward channels. Each channel is made up of one reference microphone, one secondary loudspeaker and one error microphone. The fully functional multi-channel ANC system requires data sharing between all the four reference microphones, four secondary loudspeakers and four error microphones, which will exceed the capability of a common DSP. Therefore, the minimax algorithm proposed in [13] is adopted and compared with the standard multiple-error LMS algorithm in both numerical simulations and real-time experiments based on floating-point implementations.

2. MULTI-CHANNEL ANC ALGORITHMS

The multi-channel ANC system, shown in Fig. 2, includes *I* reference microphones, *J* secondary loudspeakers and *K* error microphones, which is also called the case (I, J, K) ANC system. The reference signal vector of the *i*-th reference microphone is denoted as

$$\mathbf{x}_i(n) = [x_i(n), x_i(n-1), \cdots, x_i(n-L+1)]^T, \quad (1)$$

where *L* is the tap length for both the control filters and secondary path models. The control filter that calculates the output of the *j*-th secondary loudspeaker based on the input from the *i*-th reference microphone is denoted as

$$\mathbf{w}_{ji}(n) = \left[w_{ji}^{(0)}(n), w_{ji}^{(1)}(n), \cdots, w_{ji}^{(L-1)}(n)\right]^T. \quad (2)$$

The output of the *j*-th secondary loudspeaker is denoted as

$$\mathbf{y}_j(n) = [y_j(n), y_j(n-1), \cdots, y_j(n-L+1)]^T, \quad (3)$$

where

$$y_j(n) = \sum_{i=1}^{I} \mathbf{w}_{ji}^T(n)\mathbf{x}_i(n). \quad (4)$$

Therefore, the error signal measured at the *k*-th error microphone is a summation of the noise and anti-noise signals as

$$e_k(n) = d_k(n) + \sum_{j=1}^{J} \mathbf{s}_{kj}^T \mathbf{y}_j(n), \quad (5)$$

where $d_k(n)$ is the noise signal received by the *k*-th error microphone. The secondary path from the *j*-th secondary loudspeaker to the *k*-th error microphone is denoted as

$$\mathbf{s}_{kj} = \left[s_{kj}^{(0)}, s_{kj}^{(1)}, \cdots, s_{kj}^{(L-1)}\right]^T. \quad (6)$$

In order to update coefficients of those control filters, the standard multiple-error LMS algorithm yields

$$\mathbf{w}_{ji}(n+1) = \mathbf{w}_{ji}(n) - \mu \sum_{k=1}^{K} [e_k(n)\mathbf{x'}_{kji}(n)], \quad (7)$$

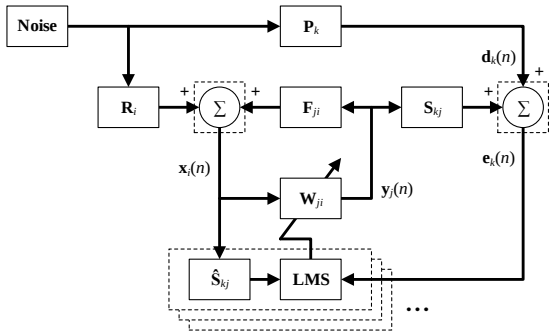

Fig. 2. Block diagram of multi-channel active noise control.

where the filtered reference signal vector is written as

$$\mathbf{x'}_{kji}(n) = \left[x'_{kji}(n), x'_{kji}(n-1), \cdots, x'_{kji}(n-L+1)\right]^T. \quad (8)$$

Each element in (8) is calculated by

$$x'_{kji}(n) = \hat{\mathbf{s}}_{kj}^T \mathbf{x}_i(n). \quad (9)$$

Here, an estimate of the secondary path assumed to be obtained offline is written as

$$\hat{\mathbf{s}}_{kj} = \left[\hat{s}_{kj}^{(0)}, \hat{s}_{kj}^{(1)}, \cdots, \hat{s}_{kj}^{(L-1)}\right]^T. \quad (10)$$

Practically, there are feedback paths from the secondary loudspeakers to the reference microphones. In our demo setup with four reference microphones and four secondary loudspeakers, there are four by four feedback paths. They can be modeled by finite impulse response (FIR) filters like the secondary paths. However, after offline modeling of the feedback paths, implementing the feedback path cancellation costs additional four by four filter operations.

Among different algorithms that reduce the computational complexity of the multi-channel ANC system, the minimax algorithm is seldom addressed after its proposal. A detailed introduction to the minimax algorithm can be found in Prof. Elliott's seminal textbook [3].

The basic idea begins by examining the cost function that the multi-channel ANC system deals with, which is given as

$$J_p = e_p = \left(\sum_{k=1}^{K} |e_k|^p\right)^{\frac{1}{p}}. \quad (11)$$

The multiple-error LMS algorithm solves this optimization problem when $p = 2$.

Another possible choice of p is to consider the ANC problem as minimizing the amplitude of the noise field, rather than the power of the noise field. This has been proven to be an efficient viewpoint, especially when the control area is relatively large. In this case, the cost function becomes

$$J_\infty = e_\infty = max\left(|e_k|\right). \quad (12)$$

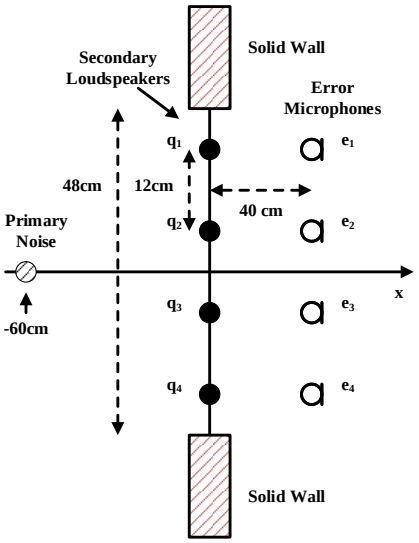

Fig. 3. Simulation setup of case (1,4,4) active noise control system.

To minimize the cost function above is same as to minimize

$$J_{\infty}^{2} = e_{\infty}^{2} = max\left(e_{k}^{2}\right). \tag{13}$$

Hence, a small modification to the multiple-error LMS algorithm will be adequate to solve the new cost function in (13). In every iteration, instead of updating coefficients of the control filters with error samples from all the error microphones, only the maximum error sample in terms of the absolute value is selected, i.e.

$$\mathbf{w}_{ji}(n+1) = \mathbf{w}_{ji}(n) - \mu e_{m}(n)\mathbf{x}'_{mji}(n), \tag{14}$$

where m is the index of the error microphone that presents the maximum absolute value.

3. NUMERICAL SIMULATION

A case (1,4,4) ANC system is configured for 2D numerical simulations, as illustrated in Fig. 3. The primary noise source is placed 60 cm from the center of the four secondary loudspeakers. The primary noise signal is generated as a random white noise and available as the common reference signal with no feedback path assumed. However, the diffraction effect of the solid walls creates unknown yet complicated primary paths. The opening between the two solid walls is 48 cm and the thickness of the walls is ignored. The error microphones are placed 40 cm away from the secondary loudspeakers. The spacing between the neighboring secondary loudspeakers, as well as between the neighboring error microphones, is set at 12 cm. The secondary path models are identified through an offline manner with 50-tap FIR filters. The control filters also have the same length of 50 taps.

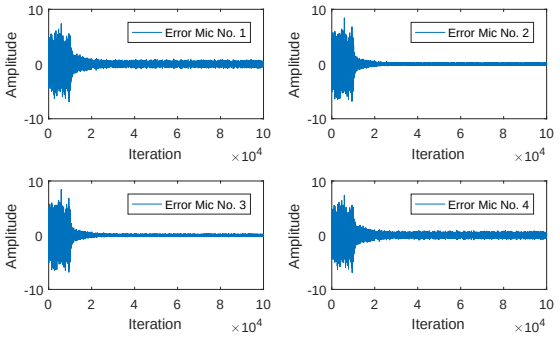

(a) Multiple-error LMS algorithm (μ = 5.0e-5)

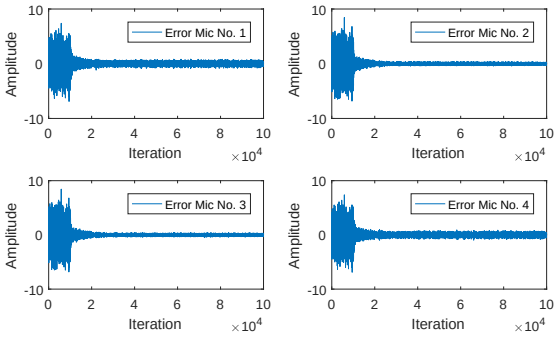

(b) Minimax algorithm (μ = 2.0e-4)

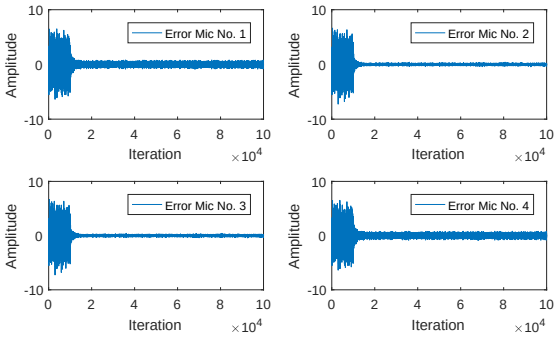

(c) Multiple-error LMS algorithm (μ = 2.0e-4)

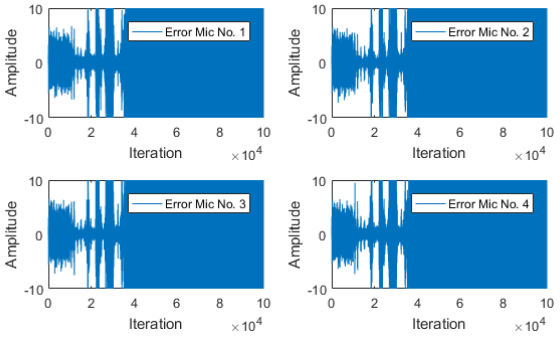

(d) Minimax algorithm (μ = 8.0e-4)

Fig. 4. Simulated outputs of error microphones.

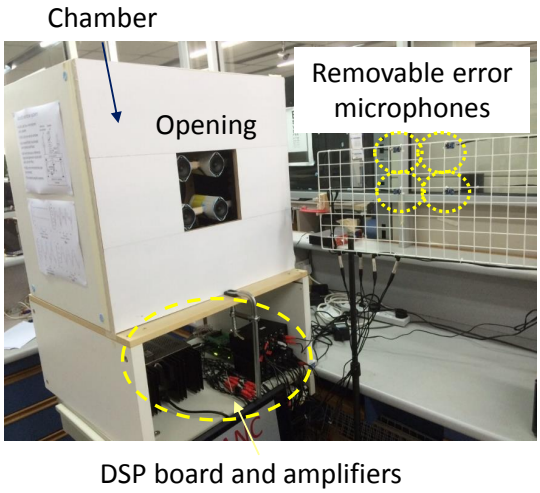

Fig. 5. Experimental setup of the 4-channel active noise canceling window.

The outputs of every error microphone are plotted in Fig. 4 using both the multiple-error LMS and minimax algorithms with different stepsize settings. When comparing Figs. 4(a) and 4(b), we note that the minimax algorithm requires four times the stepsize of the multiple-error LMS algorithm in order to achieve the same convergence speed. When using the same stepsize, the multiple-error LMS algorithm converges faster than the minimax algorithm, as shown in Figs. 4(b) and 4(c). However, the stepsize bound of the minimax algorithm doesn't appear to be broader than the multiple-error LMS algorithm. As shown in Fig. 4(d), when the stepsize is set to four times of $\mu = 2.0\text{e-}4$, the minimax algorithm cannot converge at the same speed of the multiple-error LMS algorithm using $\mu = 2.0\text{e-}4$. Instead, it diverges. Hence, although the minimax algorithm is less computationally complicated, it may slow down the convergence as a trade-off.

4. REAL-TIME EXPERIMENT

Real-time experiments are carried out with the Texas Instrument TMS320C6713 DSP starter kit running at 225 MHz clock rate. Eight ADCs and four DACs are integrated on the HEG DSK6713 IF-A data acquisition board, supporting up to 200 kHz sampling frequency and 16 bit precision. The sampling frequency used in the experiment is locked at only 16 kHz. The primary noise is enclosed in a wooden box, as shown in Fig. 5. The opening on the wooden box is 20 cm by 20 cm. The spacing between the secondary loudspeakers is 12 cm, which is also the spacing between the error microphones. Each feedforward channel obtains the reference signal from individual reference microphone, which is located at 12 cm away from the secondary loudspeaker inside the wooden box. Therefore, the feedback paths occur and affect the noise reduction performance. A band-limited white noise is used in the experiment as the primary noise.

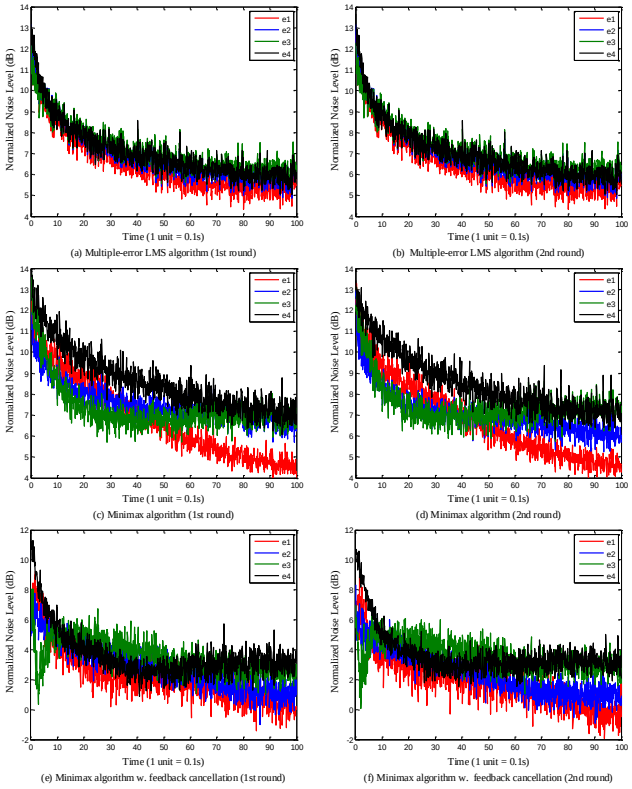

Fig. 6. Noise levels at the error microphones' locations.

When the length of the control filters is 100 taps, both the multiple-error LMS and minimax algorithms converge, without implementing the feedback path cancellation. However, the minimax algorithm remains effective when the length of the control filters increases to 120 taps and even 200 taps. The multiple-error LMS algorithm cannot run fast enough with such long tap lengths and thus breaks the causality constraint. On the other hand, the minimax algorithms allows the feedback path cancellation to be implemented when the length of the control filters is 100 taps, owing to its significant advantage in consuming less computational power. The multiple-error LMS algorithm cannot run together with the feedback path cancellation, due to the limited computational capacity of the DSP used in the experiment.

The measured convergence curves are plotted in Fig. 6. The multiple-error LMS algorithm tends to converge to the same level at all the four error microphones' locations, as shown in Fig. 6(a). In contrast, the minimax algorithm converges to different levels at the error microphones' locations. It is likely that the recording duration is insufficient to show the complete convergence of the minimax algorithm, as the minimax algorithm converges slower than the multiple-error LMS algorithm. Furthermore, Fig. 6(c) shows that the benefit of the feedback cancellation is an additional 2-3 dB noise re-

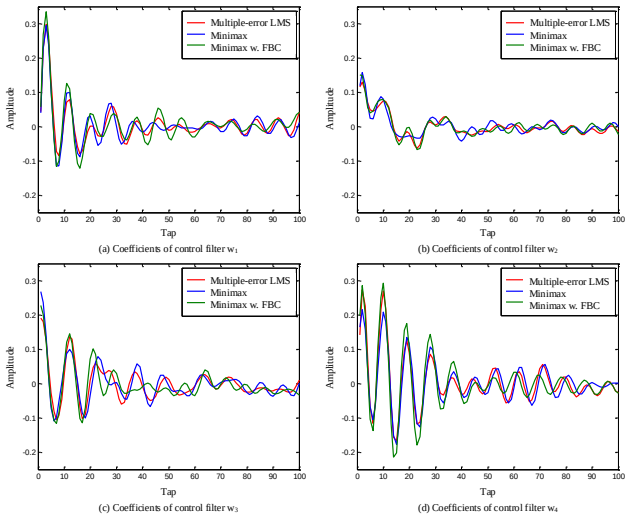

Fig. 7. Converged control filters in the experiment.

duction, due to the fact that higher quality of reference signals leads to better performance of ANC systems.

The coefficients of the control filter after convergence are plotted in Fig. 7. The multiple-error LMS algorithm results in similar control filters as the minimax algorithm. This is partially because the configuration of the 4-channel active noise canceling window is symmetric. When the gains of the amplifiers are uniform, the control filters can be the same across all channels [9]. When the feedback path cancellation is implemented, the control filters are different from those obtained without feedback path cancellation, since the primary paths have been changed implicitly.

5. CONCLUSIONS

This paper revisits the minimax algorithm specifically for a new application of the multi-channel ANC system, namely the active noise canceling window. As compared to the multiple-error LMS algorithm, the minimax algorithm updates coefficients of the control filters by only one error sample in every iteration. The saved computational power can be relocated for longer tap lengths or the feedback path cancellation so that better noise reduction performance can be achieved. However, the minimax algorithm converges slower than the multiple-error LMS algorithm when the same stepsize is used. It will be interesting to investigate different approaches to accelerate the convergence of the minimax algorithm in future works.

6. REFERENCES

[1] P. Lueg, "Process of silencing sound oscillations," US Patent 2043416, 1936.

[2] L. J. Eriksson, "Development of the filtered-U algorithm for active noise control," *J. Acoust. Soc. Amer.*, vol. 89, no. 1, pp. 257-265, 1991.

[3] S. J. Elliott, *Signal processing for active control*. Academic Press: London, 2000.

[4] C. H. Hansen, *Understanding active noise cancellation*. Spon Press: London, 2001.

[5] Y. Kajikawa, W. S. Gan, and S. M. Kuo, "Recent advances on active noise control: Open issues and innovative applications," *APSIPA Trans. Sig. Inf. Process.*, vol. 1, no. e3, pp. 1-21, 2012.

[6] B. Lam, C. Shi, and W. S. Gan, "Active noise control systems for open windows: Current updates and future perspectives," *Proc. 24th Int. Congr. Sound Vib.*, London, UK, 2017.

[7] T. Murao, C. Shi, W. S. Gan, and M. Nishimura, "Mixed-error approach for multi-channel active noise control of open windows," *Applied Acoust.*, vol. 127, pp. 305-315, 2017.

[8] B. Lam, J. He, T. Murao, C. Shi, W. S. Gan, and S. Elliott, "Feasibility of the full-rank fixed-filter approach in the active control of noise through open windows," *Proc. 45th Int. Congr.Expo. Noise Control Eng. (INTER-NOISE)*, Hamburg, Germany, 2016.

[9] T. Murao and M. Nishimura, "Basic study on active acoustic shielding," *J. Environment Eng.*, vol. 7, no. 1, pp.76-91, 2012.

[10] T. Murao, M. Nishimura, K. Sakurama, S. Nishida, "Basic study on active acoustic shielding: Improving the method to enlarge the AAS window," *Mechanical Eng. J.*, vol. 3, no. 1, pp. 1-12, 2016.

[11] B. Lam and W. S. Gan, "Active acoustic windows: Towards a quieter home," *IEEE Potentials* vol. 35, no. 1, pp. 11-18, 2016.

[12] S. Ise, "The boundary surface control principle and its applications," *IEICE Trans. Fundamentals*, vol. E88-A, no. 7, pp. 1656-1664, 2005.

[13] A. Gonzales, A. Albiol, and S. J. Elliott, "Minimization of the maximum error signal in active control," *IEEE Trans. Speech Audio Process.*, vol. 6, no. 3, pp. 268-281, 1998.

[14] S. J. Elliott, I. M. Stothers, and P. A. Nelson, "A multiple error LMS algorithm and its application to the active control of sound and vibration," *IEEE Trans. Acoust. Speech Sig. Process.*, vol. ASSP-35, no. 10, 1987.